

# The XUV monochromator for ultrashort pulses at the Artemis facility

Contact [poletto@dei.unipd.it](mailto:poletto@dei.unipd.it)

**L. Poletto, S. Bonora, F. Frassetto and P. Villorosi**

CNR-National Institute for the Physics of Matter and Dep.t of Information Engineering, Univ. of Padova  
Via Gradenigo 6/B, Padova (Italy)

**E. Springate, C. A. Froud, I. C. E. Turcu, D. S. Wolff and J. S. Collier**

Central Laser Facility, STFC, Rutherford Appleton Laboratory, HSIC, Didcot, Oxon OX11 0QX, UK

**M. Roper**

STFC, Daresbury Laboratory, Daresbury Science & Innovation Campus, Warrington, Cheshire WA4 4AD, UK

## Introduction

Artemis is a multi-disciplinary facility based on high-repetition-rate and few-optical-cycle tuneable laser sources, one of which is used to produce ultrafast extreme-ultraviolet (XUV) pulses through high-order harmonic (HH) generation. The XUV beam is delivered to the interaction stations in two beamlines, one for broad-band and one for monochromatised XUV pulses. Here, we present the design and characterization of the XUV grating monochromator of Artemis. Aim of the instrument is the spectral selection of XUV HHs with high throughput and short temporal broadening in the 15-100 eV (12-82 nm). This is achieved through an innovative optical design using gratings in the off-plane mount. The preliminary results achieved at Artemis will be also presented.

## Monochromator design

The monochromator adopts gratings in the off-plane mount: it differs from the classical one in that the incident and diffracted wave vectors are almost parallel to the grooves<sup>[1]</sup>. The grating geometry and a schematic of the monochromators are shown in Fig. 1.

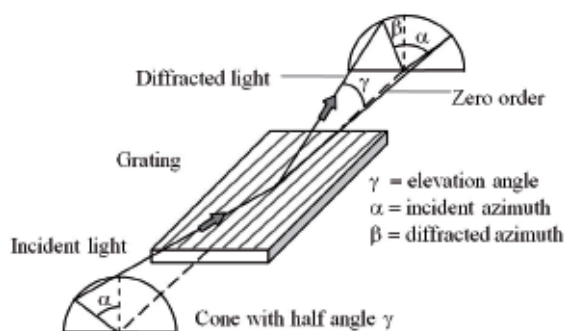


**Figure 1. The geometry of the off-plane mount.**

The geometry is described by two angles, the altitude and the azimuth. The elevation  $\gamma$  is the angle between the direction of the incoming rays and the direction of the rulings and defines the half-angle of the cone into which the light is diffracted. The azimuth  $\alpha$  is defined to be zero if the rays lie in the plane perpendicular to the grating surface and parallel to the rulings. Let  $\beta$

define the azimuth of the diffracted light at wavelength  $\lambda$  and order  $m$ . The grating equation is then written as

$$\sin\gamma (\sin\alpha + \sin\beta) = m\lambda\sigma \quad (1)$$

where  $\sigma$  is the groove density. The blaze condition for maximum efficiency is defined when the surface of each grating groove is seen by the incident ray as a plane mirror, that is  $\alpha = \beta = \delta$ , where  $\delta$  is the groove blaze angle. It has been theoretically demonstrated and experimentally measured that the efficiency of a grating used in such geometry is close to the reflectivity of the coating at the same altitude angle, so much higher efficiencies than the classical mount can be obtained in the XUV<sup>[2]</sup>.

The schematic of a monochromator is shown in Fig. 2: it adopts a plane grating and two concave mirrors. The first mirror collimates the light coming from the source, the grating is operated at first diffraction order in parallel light in the condition  $\alpha = \beta$ , then the second mirror focuses the diffracted light on the exit slit. The wavelength scanning is provided by rotating the grating around an axis passing through the grating center and parallel to the groove direction, following the equation

$$2 \sin\gamma \sin\alpha = \lambda\sigma. \quad (2)$$

The azimuth changes with the wavelength while the elevation is kept constant, so that the maximum efficiency condition is fulfilled at the blaze wavelength  $\lambda_B = 2 \sin\gamma \sin\delta/\sigma$ . At different wavelengths, the efficiency decreases. Nevertheless, it has been shown that this mounting is very efficient in a broad spectral region for the spectral selection of HHs<sup>[3]</sup>.

The design parameters are resumed in Table 1. The instrument is operated without an entrance slit, since the size of the HH source is very small, in the 15-30  $\mu\text{m}$  range. Four different gratings are mounted to cover with low or medium resolution the 15-100 eV spectral region at elevation of  $3.5^\circ$ . The grating selection is made by a motorized mechanism. The spectral scans are performed through the grating rotation<sup>[4]</sup>. It is possible also to insert a plane mirror in the collimated part of the monochromator instead of a grating, so the instrument acts as a relay section without any spectral selection.

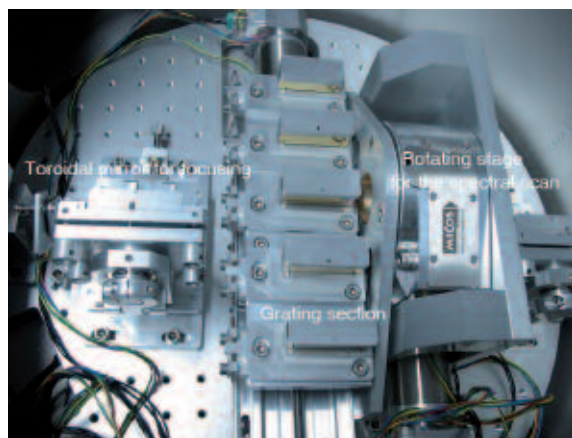
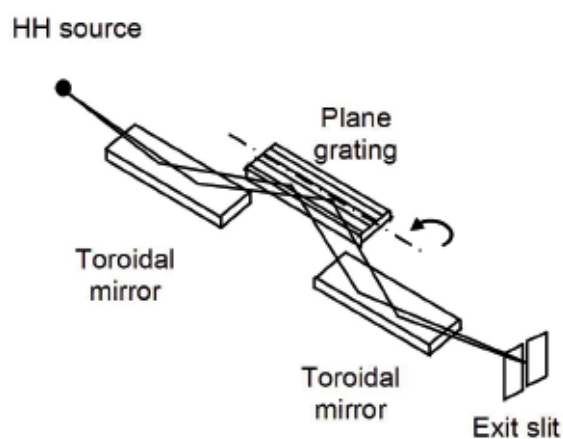


Figure 2. Schematic of the monochromators (upper part) and internal view of the instrument with the four grating and the two toroidal mirrors (lower part).

The temporal duration of an ultrafast pulse is increased when it is subject to the spectral dispersion given by a grating. This is due to two mechanisms. The first is the filtering of the pulse spectrum that occurs during monochromatization. This effect is negligible for HH radiation if the complete spectral extension of a single harmonic is selected by the monochromator. The major mechanism responsible for the temporal broadening is the difference in the lengths of the optical paths of the rays diffracted by different grating grooves. Indeed, the spectral phase of the XUV pulse results chirped, similarly to the conventional laser stretcher operating in the visible and near infrared. The total difference in the optical paths of the rays diffracted by  $N$  grooves illuminated by radiation at wavelength  $\lambda$  is  $Nm\lambda$ . This effect is important in the femtosecond time scale and has to be taken into account when planning the use of a grating monochromator for ultrafast pulses. The temporal broadening given by the monochromator is shown in Table 1 for a source with 8 mrad divergence, that is the acceptance angle of the monochromator. In the case of the low-resolution gratings, the broadening is expected to be of the order of 10 fs. The use of the off-plane geometry minimizes the number of illuminated grooves for a given resolution with respect to the classical mount, then the grating temporal response is shorter.

### Grating 1 and 3 12-40 eV region (30-100 nm)

G1 60 gr/mm,  $\Delta\lambda = 2.8$  nm,  $\Delta T = 10$  fs @27 eV

G3 300 gr/mm,  $\Delta\lambda = 0.6$  nm,  $\Delta T = 55$  fs @27 eV

### Grating 2 and 4 35-100 eV region (12-35 nm)

G2 120 gr/mm,  $\Delta\lambda = 1.4$  nm,  $\Delta T = 10$  fs @72 eV

G4 500 gr/mm,  $\Delta\lambda = 0.3$  nm,  $\Delta T = 35$  fs @72 eV

Table 1. Grating parameters. The bandwidth  $\Delta\lambda$  is calculated on a  $50 \mu\text{m}$  slit, the temporal response  $\Delta T$  with a source with 8 mrad divergence.

## Monochromator characterization in Padova

The calibration of the spectral response has been performed in the CNR-INFM Laboratory for UV and X-ray Optical Research (LUXOR) in Padova (Italy) a hollow cathode lamp in the 12-50 eV (25-100 nm) interval and a microfocus X-ray source in the 50-100 eV (12-25 nm) interval. Some spectra are shown in Fig. 3. The width of the spectral lines is limited by the slit width, confirming that the spectral aberrations of the optical system are negligible.

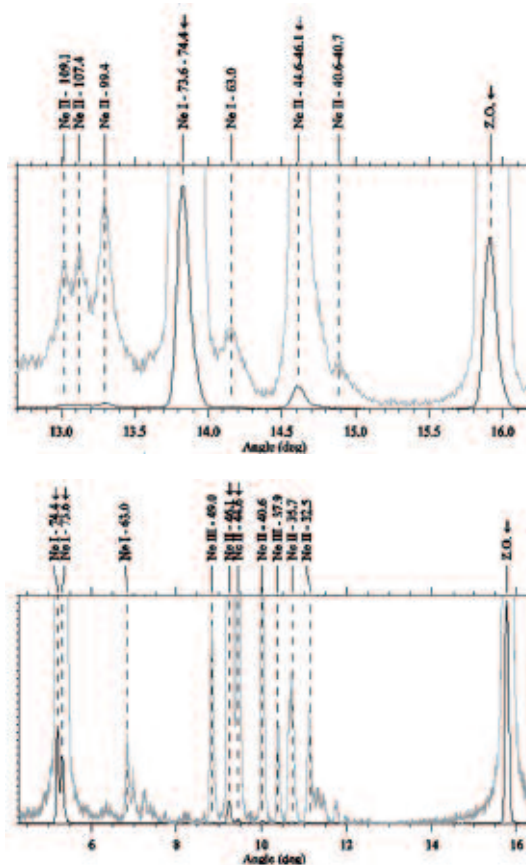


Figure 3. Some calibration spectra taken in Padova: a) hollow-cathode source, G1; b) hollow-cathode source, G3. The over-imposed plots refer to spectral lines with lower intensities. Note the different spectral resolution between the two gratings.

Also the global efficiency of the monochromator, which includes the mirror reflectivity and the grating efficiency, has been measured in Padova. The results are reported in Table 2.

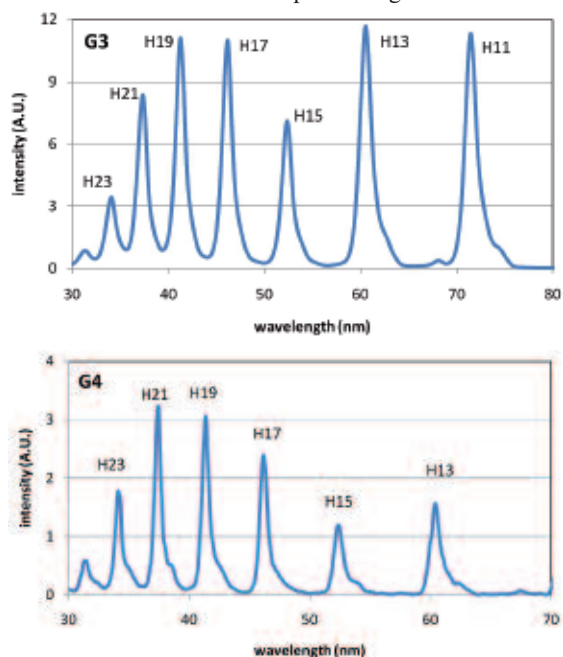
G1	0.21 @27 eV (46 nm)
G3	0.24 @27 eV (46 nm)
G2	0.26 @72 eV (17 nm) 0.28 @72 eV (17 nm)

**Table 2. Monochromator efficiency at the blaze wavelength.**

### Monochromator characterization at Artemis

The monochromator has been installed at Artemis in November 2008. The instrument has been aligned and characterized in terms of wavelength calibration and absolute photon throughput.

The HHs were generated by 1-mJ 25-fs Ti:Sa laser pulses at 1 kHz repetition rate. The laser was focused in the gas jet by a 30-cm lens. The jet was injected into the generation chamber through a piezoelectric valve operated at the laser repetition rate. The HH spectra have been acquired through the grating rotation on a channel-electron-multiplier detector. Argon and neon was used as the interacting medium to generate harmonics in the 30-80 nm spectral region. Some



spectra are shown in Fig. 4.

**Figure 4. Some HH spectra generated in argon taken at Artemis: a) G3; b) G4.**

Finally, the absolute response, intended here as the absolute number of photon throughput from the exit slit, was measured by a calibrated aluminum photodiode. The results obtained in argon are reported in Table 3. The output flux is in the range  $10^7$ - $10^9$  ph/s in the 32-72 nm (17-39 eV) range, the highest flux being at the long wavelengths. Using neon, the flux is reduced by about one order of magnitude.

Wavelength (nm)	G1 (ph/shot)	G2 (ph/shot)	G3 (ph/shot)	G4 (ph/shot)
71.4 (H11)	$1 \cdot 10^6$	$1 \cdot 10^5$	$5 \cdot 10^5$	$7 \cdot 10^4$
60.4 (H13)	$8 \cdot 10^5$	$1 \cdot 10^5$	$5 \cdot 10^5$	$6 \cdot 10^4$
52.3 (H15)	$5 \cdot 10^5$	$1 \cdot 10^5$	$4 \cdot 10^5$	$1 \cdot 10^5$
46.2 (H17)	$6 \cdot 10^5$	$2 \cdot 10^5$	$6 \cdot 10^5$	$2 \cdot 10^5$
41.3 (H19)		$2 \cdot 10^5$	$6 \cdot 10^5$	$2 \cdot 10^5$
37.4 (H21)		$2 \cdot 10^5$	$5 \cdot 10^5$	$1 \cdot 10^5$
34.1 (H23)			$2 \cdot 10^5$	$3 \cdot 10^4$
31.4 (H25)			$5 \cdot 10^4$	$1 \cdot 10^4$

**Table 3. Monochromator throughput with HHs generated in argon. The flux is measured as the output from a 50  $\mu$ m-wide exit slit.**

### Conclusions

The monochromator for Artemis is operative in the monochromatic beamline since December 2008. It has been characterized in terms of wavelength calibration and absolute response. In the present setup, it gives at the output  $10^7$  to  $10^9$  ph/s in the 32-72 nm range.

The authors would like to thank the technical staff at Rutherford Appleton Laboratory for the support received during the installation of the monochromator at Artemis.

### References

1. W. Cash, *Appl. Opt.*, **21**, 710 (1982).
2. M. Pascolini *et al.*, *Appl. Opt.*, **45**, 3253 (2006).
3. L. Poletto *et al.*, *Opt. Lett.*, **32**, 2897 (2007).
4. F. Frassetto *et al.*, *SPIE Proc.*, **7077**, 707713 (2008).